CALCULATION METHOD FOR FIN-AND-TUBE HEAT EXCHANGERS OPERATING WITH NONUNIFORM AIRFLOW

PAOLO BLECICH, ANICA TRP & KRISTIAN LENIĆ
Faculty of Engineering, University of Rijeka, Croatia

ABSTRACT

This paper presents a new calculation method for fin-and-tube heat exchangers operating with nonuniform airflow. The calculation method consists of discretizing the heat exchanger tubes into tube elements and applying mass and energy conservation equations. The calculation method is capable of predicting local and overall values of thermal effectiveness, heat transfer rates and fluid outlet temperatures in fin-and-tube heat exchangers subject to airflow nonuniformity. The results of the tube element method are compared against experimental data, and good accordance has been achieved between predicted and measured values. Experimental data is collected for fin-and-tube heat exchangers placed inside an open wind tunnel, where airflow nonuniformity is generated by partially obstructing the entrance cross section. This study revealed that airflow nonuniformity causes effectiveness deterioration in fin-and-tube heat exchangers. The exact value of effectiveness deterioration depends on the heat exchanger dimensionless groups – the number of heat transfer units (NTU) and the heat capacity rate ratio (C^*) – as well as on the intensity and orientation of the airflow nonuniformity. The design of the tube-side fluid circuitry, which affects the heat exchanger flow arrangement, also plays a role in the effectiveness deterioration. The tube element method revealed that the effectiveness deterioration increases with the intensity of airflow nonuniformity. For an observed nonuniform airflow profile, the effectiveness deterioration is maximum in heat exchangers with a balanced heat capacity rate ratio ($C^* = 1$) and minimum in evaporators and condensers ($C^* = 0$).

Keywords: fin-and-tube heat exchanger, airflow nonuniformity, effectiveness deterioration, calculation method.

1 INTRODUCTION

Fin-and-tube heat exchangers find extensive application in the building sector, in the transport, process and power industries. The inlet airflow distribution strongly affects the performance of fin-and-tube heat exchangers. Nonuniform airflow distribution or airflow nonuniformity causes loss of thermal performance in heat exchangers. Airflow nonuniformity may be induced by poor design of the inlet header, adverse operating conditions, vicinity of the blower, fouling or geometrical irregularities on the heat exchanger surfaces, as stressed by Kitto and Robertson [1], Mueller and Chiou [2], and Shah and Sekulić [3]. Generally, sizing and calculation methods for fin-and-tube heat exchanger assume uniform airflow over the entire heat exchanger surface.

Airflow nonuniformity negatively affects the thermal and hydraulic performance of fin-and-tube heat exchangers, see Singh et al. [4]. The loss of thermal performance is represented by a reduction of the heat flow rate and thermal effectiveness of the heat exchanger. Based on a review of the literature, the general conclusion is that the thermal performance deterioration depends on the number of heat transfer units (NTU), the heat capacity rate ratio (C^*), the tube-side fluid circuitry, the intensity and orientation of the airflow nonuniformity. Furthermore, it was seen that the thermal performance deterioration is higher in heat exchangers with balanced heat capacity rates ($C^* = 1$) than in evaporators and condensers ($C^* = 0$), as referred by Ranganayakulu and Seetharamu [5].

www.witpress.com, ISSN 1743-3541 (on-line)
doi:10.2495/ESUS190021

Experimental, analytical and numerical methods have been extensively used to investigate the effect of nonuniform airflow on the performance of fin-and-tube heat exchangers, see Domanski and Yashar [6], Mao et al. [7] and Ranganayakulu and Seetharamu [8]. Generally, nonuniform airflow causes effectiveness deterioration in the range between between 5 and 15%, as stated by Bahman and Groll [9] and Hajabdollahi and Seifoori [10]. The effectiveness deterioration can be even higher, up to 30%, if nonuniform airflow causes refrigerant maldistribution on the tube side, as concluded by Yashar et al. [11]. Generally, the abovementioned research are limited to simple one-dimensional nonuniform airflow profiles or provide data for specific heat exchangers.

This paper presents a new method for the calculation of the thermal performance of fin-and-tube heat exchangers operating in nonuniform airflow, which can be also used for two-dimensional nonuniform airflow profiles. Section 2 shows the analysed heat exchanger, describes the experimental and analytical approaches while Section 3 presents the validation and the results obtained with the presented analytical method.

2 METHODOLOGY

2.1 The fin-and-tube heat exchanger

The analysed fin-and-tube heat exchanger is a three-row heat exchanger with a total 38 tubes, distributed into seven flow circuits (HEX:3R-7C). The seven flow circuits have different number of passes: five flow circuits have a six-pass arrangement and two flow circuits have a four-pass arrangement, as shown in Fig. 1. It can be observed that the fin-and-tube heat exchanger exhibits a Z-shaped flow circuitry on the tube side causing water to flow back-and-forth between the first and third tube row.

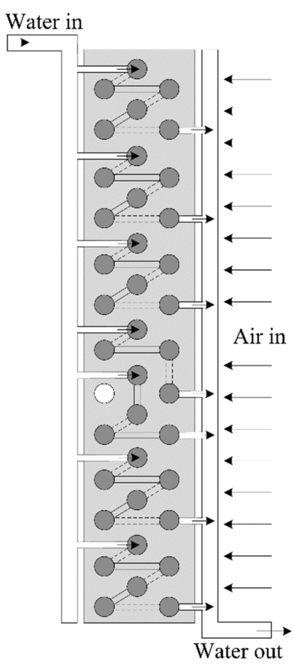

Heat exchanger	HEX:3R-7C
Overall height, mm	840
Overall length, mm	760
Overall depth, mm	155
Tube fluid flow length, mm	700
Fin depth, mm	90
Fin height, mm	780
Number of fins, -	260
Fin pitch, mm	2.6
Fin thickness, mm	0.2
Fin type	flat plain
Fin material	aluminum
Air-side heat transfer area, m^2	40
Surface compactness, m^2/m^3	814
Number of rows	3
Transverse tube pitch, mm	60
Longitudinal tube pitch, mm	30
Outer tube diameter, mm	15.9
Inner tube diameter, mm	14.8
Tube material	copper

Figure 1: Geometry and tube-side flow circuitry of the HEX:3R-7C heat exchanger.

2.2 Experimental method

The experimental setup consists of an open wind tunnel, the heat exchanger test section equipped with temperature and air velocity measurement sensors and a data acquisition system. The experimental setup is shown in Fig. 2.

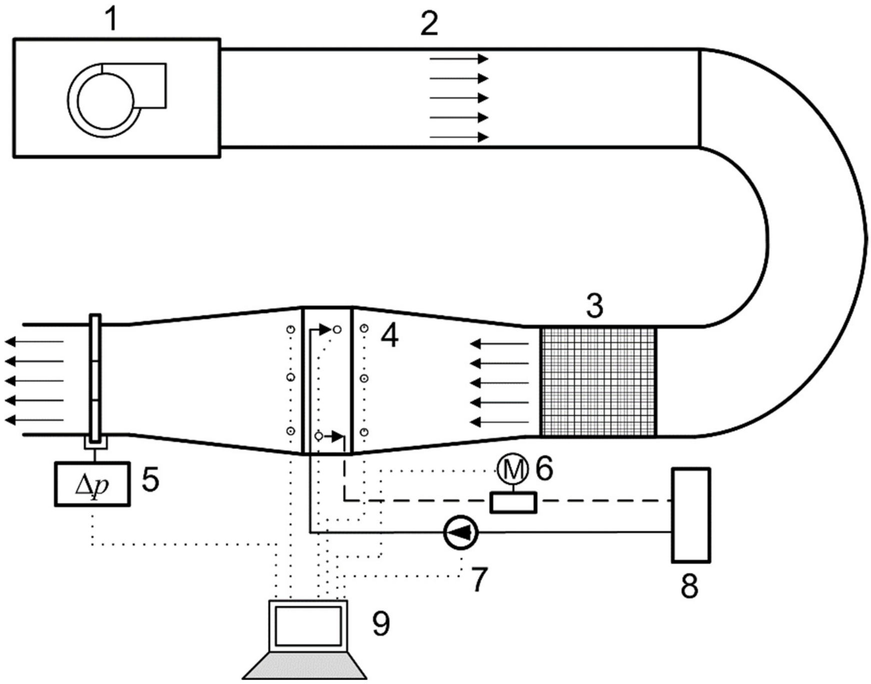

Figure 2: The open wind tunnel. 1: Blower; 2: Air ducts; 3: Flow straightener; 4: Heat exchanger test section; 5: Orifice; 6: Water mass flow meter; 7: Water pump; 8: Heat source; 9: Data acquisition.

The fin-and-tube heat exchanger is placed inside the test section. The air mass flow rate was determined from the pressure drop generated through a calibrated orifice. The water mass flow rate flowing through the heat exchanger pipes was measured using an ultrasound mass flow meter. K-type thermocouples were placed across the heat exchanger inlet and outlet cross section in order to measure the inlet and outlet air temperatures. Inlet and outlet water temperatures were measured using Pt100 temperature sensors.

The placement of the temperature sensors is shown in Fig. 3(a) and (b). Uniform airflow was obtained by leaving the inlet cross section unobstructed, Fig. 3(c), while nonuniform airflow was generated by placing screen and partially obstructing the inlet cross section, as shown in Fig. 3(d)–(f). The water mass flow rate was in the range between 800 and 3200 kg/h, while the air mass flow rate was 1650 kg/h. The air inlet temperature was 15°C while the water inlet temperature was 60°C. The combined uncertainty of all measurements was estimated to be within ±3.0% at 95% confidence level. The average exchanger heat transfer rate ($\dot{Q}_m$) in the fin-and-tube heat exchanger is calculated from the arithmetic mean of the heat transfer rates measured on the air side ($\dot{Q}_a$) and on the water side ($\dot{Q}_w$):

$$\dot{Q}_{\mathrm{m}} = \frac{\dot{Q}_{\mathrm{a}} + \dot{Q}_{\mathrm{w}}}{2}. \tag{1}$$

The heat exchanger effectiveness (ε) is the ratio of the actual heat transfer rate ($\dot{Q}_{\mathrm{m}}$) to the maximum theoretical heat transfer rate ($\dot{Q}_{\mathrm{max}}$):

$$\varepsilon = \frac{\dot{Q}_{\mathrm{m}}}{\dot{Q}_{\mathrm{max}}} = \frac{\dot{Q}_{\mathrm{a}} + \dot{Q}_{\mathrm{w}}}{2\,\dot{m}_{\mathrm{a}}\, c_{\mathrm{a}} \left(T_{\mathrm{w,in}} - T_{\mathrm{a,in}}\right)}. \tag{2}$$

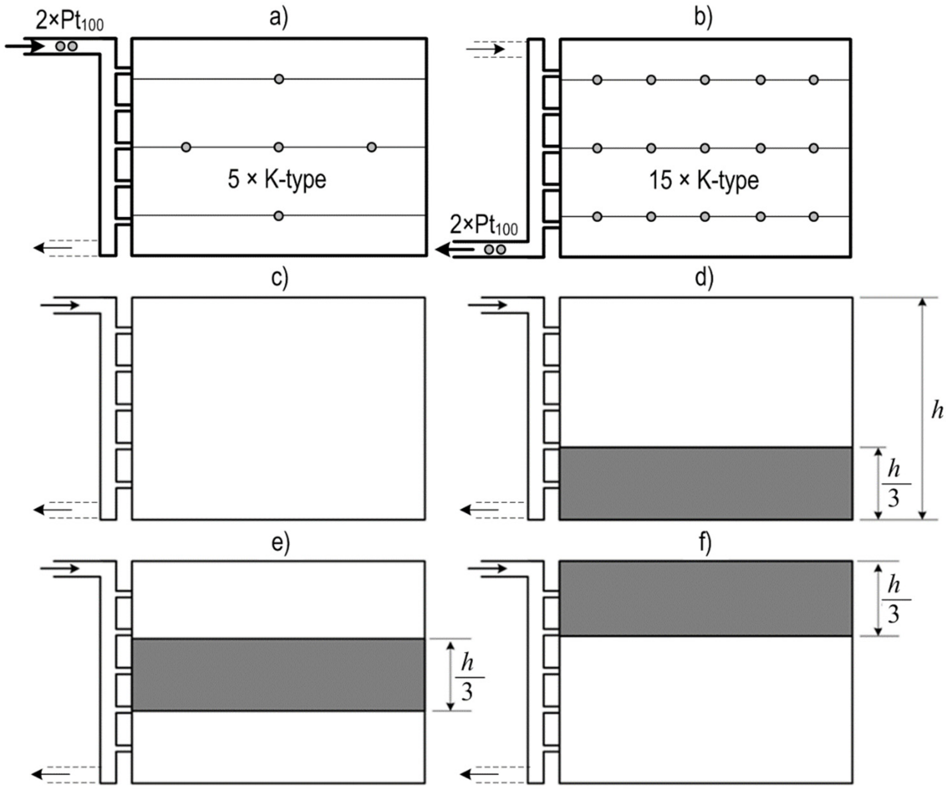

Figure 3: The fin-and-tube heat exchanger setup. (a) Temperature sensors at the air inlet cross section; (b) Temperature sensors at the air outlet cross section; (c) Unobstructed inlet – uniform airflow; (d)–(f) Obstructed inlet with screens – nonuniform airflows, profiles A1, A2 and A3, respectively.

The air and water mass flow rates are $\dot{m}_{\mathrm{a}}$ and $\dot{m}_{\mathrm{w}}$ while the air and water inlet temperatures are $T_{\mathrm{a,in}}$ and $T_{\mathrm{w,in}}$, respectively. The air and water specific heat capacities are c_{a} and c_{w}. Heat exchangers operating under nonuniform airflow are subject to a loss of thermal performance that can be expressed as effectiveness deterioration. The effectiveness deterioration ($\Delta\varepsilon$) is the relative difference between the heat exchanger effectiveness operating in uniform airflow ($\varepsilon_{\mathrm{uniform}}$) and the heat exchanger effectiveness operating in nonuniform airflow ($\varepsilon_{\mathrm{nonuniform}}$):

$$\Delta\varepsilon = \frac{\varepsilon_{\text{uniform}} - \varepsilon_{\text{nonuniform}}}{\varepsilon_{\text{uniform}}} \cdot 100\% . \tag{3}$$

2.3 Analytical method

The most widely used thermal design method for fin-and-tube heat exchangers is the effectiveness-number of transfer units method (ε-*NTU* method). In this method, the heat exchanger is defined by three independent dimensionless groups: (1) the thermal effectiveness (ε); (2) the number of transfer units (*NTU*); and (3) the heat capacity rate ratio (C^*). Thus, the heat exchanger effectiveness depends on the dimensionless groups *NTU* and C^* but also on the fluid flow arrangement:

$$\varepsilon = f\left(NTU = \frac{U \cdot A}{C_{\min}},\ C^* = \frac{C_{\min}}{C_{\max}},\ \text{fluid flow arrangement} \right). \tag{4}$$

Mathematical expressions for the heat exchanger effectiveness are available for simple fluid flow arrangements, such as the counterflow, the parallelflow and the crossflow:

$$\text{counterflow:} \begin{cases} \varepsilon = \dfrac{1-\exp\left[-NTU(1-C^*)\right]}{1-C^*\exp\left[-NTU(1-C^*)\right]}, & \text{for } 0 \le C^* < 1 \\ \varepsilon = \dfrac{NTU}{1+NTU}, & \text{for } C^* = 1 \end{cases}, \tag{5}$$

$$\text{parallelflow:} \quad \varepsilon = \frac{1-\exp\left[-NTU(1+C^*)\right]}{1+C^*}, \tag{6}$$

$$\text{crossflow:} \quad \varepsilon = 1-\exp\left\{ \frac{NTU^{0.22}\left[\exp(-NTU^{0.78}C^*)-1\right]}{C^*} \right\}. \tag{7}$$

It should be noted that the effectiveness of the crossflow heat exchanger is expressed by the Eckert approximation (eqn (7)), which deviates from the exact Nusselt solution by ±3%. For single-pass crossflow fin-and-tube heat exchangers with less than 4 tube rows the Eckert formula overestimates the heat exchanger effectiveness. For a single-pass three tube row heat exchanger with $C_{\min}$ on the air-side [12] the following expression applies:

$$\left.\begin{array}{l}\text{single-pass three} \\ \text{tube row crossflow}\end{array}\right\} \begin{array}{c} \varepsilon = \left\{1-\exp(-3KC^*)\left[1+C^*K^2(3-K)+3C^{*2}K^4/2\right]\right\}/C^* \\ K = 1-\exp(-NTU/3) \end{array} . \tag{8}$$

The analysis becomes increasingly difficult for complex fluid flow arrangement and analytical solutions are available for a limited number of arrangements, as provided by Bačlić and Gvozdenac [13], but often include infinite series and complex mathematical functions. Boundary conditions, specifically the mass flow rates and inlet temperatures of the two fluids, are necessary to achieve closure in ε-*NTU* equations.

The heat capacity rate ratio (C^*) is easily determined from the mass flow rates and specific heat capacities of the two fluids, but calculation of the number of transfer units ($NTU = UA/C_{\min}$) is more complex since it includes the overall thermal conductance (*UA*), which is the product of the overall heat transfer coefficient (*U*) and the total heat transfer area (*A*):

$$UA=\left[\frac{1}{(\eta hA)_\mathrm{a}}+\frac{\ln(d_\mathrm{o}/d_\mathrm{i})}{2\pi(kLN)_\mathrm{t}}+\frac{1}{(hA)_\mathrm{w}}\right]^{-1}. \tag{9}$$

The water heat transfer coefficient (h_w) is calculated using the correlation of Gnielinski [14], and the air-side heat transfer coefficient (h_a) is determined from the Wang et al. [15] correlation for the Colburn j factor. The surface efficiency on the air-side (η_a) is determined from the Schmidt approximation method [16].

A fin-and-tube heat exchanger with complex fluid flow arrangement and nonuniform fluid temperatures and velocities at the inlet can be analysed by the tube element method (TEM). In the tube element method, the fin-and-tube heat exchanger is discretized into tube elements, on which mass and energy conservation equations can be applied. At the entrance of each tube element, the fluid flow velocities and temperatures are assumed uniform. By performing a fine discretization it can be assumed that the heat capacity rate of the tube-side is much bigger than the heat capacity rate of the air-side ($C_\mathrm{min,el}$ / $C_\mathrm{max,el} \approx 0$). This is a fair assumption, especially when the tube side fluid is water or a refrigerant. In that case, the thermal effectiveness of the element can be determined as the thermal effectiveness of an ideal evaporator or condenser.

Another assumption is that the tube-side fluid temperature changes linearly along the tube element. In that case the average temperature of the tube-side fluid is the arithmetic mean of the inlet and outlet temperatures at the tube element. Fig. 4 shows the idea behind the tube element method. For the observed tube element, the air mass flow rate is denoted with $\dot{m}_\mathrm{a,el}$, the inlet and outlet air temperature with $T_\mathrm{a,el,in}$ and $T_\mathrm{a,el,out}$. On the tube side, the water mass flow rate is denoted with $\dot{m}_\mathrm{w,el}$, the inlet and outlet water temperatures with $T_\mathrm{w,el,in}$ and $T_\mathrm{w,el,out}$.

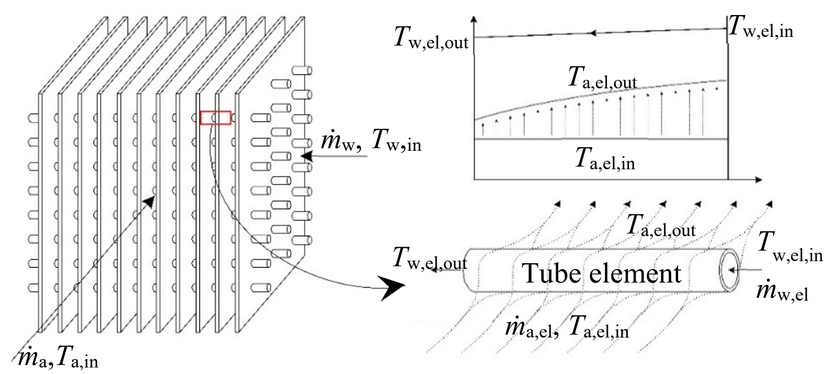

Figure 4: The fin-and-tube heat exchanger and its discretization into tube elements.

The heat balance equation for an observed tube element is written as:

$$\dot{m}_\mathrm{a,el}\,c_\mathrm{a}\left(T_\mathrm{a,el,out}-T_\mathrm{a,el,in}\right)=\dot{m}_\mathrm{w,el}\,c_\mathrm{w}\left(T_\mathrm{w,el,in}-T_\mathrm{w,el,out}\right). \tag{10}$$

The air and water mass flow rates at the tube element are $\dot{m}_\mathrm{a,el}$ and $\dot{m}_\mathrm{w,el}$. The air and water inlet and outlet temperatures are $T_\mathrm{a,el,in}$, $T_\mathrm{a,el,out}$, $T_\mathrm{w,el,in}$, $T_\mathrm{w,el,out}$, respectively. The heat capacity rate ratio for the tube element (C_el*) is calculated from:

$$C_{\mathrm{el}}^{*} = \frac{\dot{m}_{\mathrm{a,el}}\, c_{\mathrm{a}}}{\dot{m}_{\mathrm{w,el}}\, c_{\mathrm{w}}} \quad . \tag{11}$$

Under nonuniform airflow conditions, each of the tube elements is exposed to different air mass flow rates. In that case, the air mass flow rate at the tube elements can be expressed using the continuity equation:

$$C_{\mathrm{el}}^{*} = \frac{w_{\mathrm{a,el}} A_{\mathrm{a}} \rho_{\mathrm{a}} c_{\mathrm{a}}}{\dot{m}_{\mathrm{w,el}} c_{\mathrm{w}}} \quad . \tag{12}$$

In the above equation, the air velocity at the tube element is $w_{\mathrm{a,el}}$, the tube element cross section is A_{a} and the air density ρ_{a}. On the tube-side the water mass flow rate at the tube element is determined by dividing the total water mass flow rate by the number of tube circuits, assuming that the water flow is uniformly distributed among them. The number of transfer units of the tube element (NTU_{el}) is determined from:

$$NTU_{\mathrm{el}} = \frac{UA_{\mathrm{el}}}{C_{\mathrm{a}}} = \frac{UA_{\mathrm{el}}}{w_{\mathrm{a,el}} A_{\mathrm{a}} \rho_{\mathrm{a}} c_{\mathrm{a}}} \quad . \tag{13}$$

The tube element effectiveness ($\varepsilon_{\mathrm{el}}$) is calculated assuming that $C^* = 0$, that is:

$$\varepsilon_{\mathrm{el}} = 1 - \exp(-NTU_{\mathrm{el}}) \ . \tag{14}$$

The air and water temperatures at the outlet of the tube element can be determined from the system of equations comprising the tube element heat balance (eqn (10)) and the tube element dimensionless groups (eqns (12)–(14)):

$$\begin{aligned} T_{\mathrm{w,el,out}} &= \frac{(2-\varepsilon_{\mathrm{el}} C_{\mathrm{el}}^{*}) T_{\mathrm{w,el,in}} + 2\varepsilon_{\mathrm{el}} C_{\mathrm{el}}^{*} T_{\mathrm{a,el,in}}}{2+\varepsilon_{\mathrm{el}} C_{\mathrm{el}}^{*}} \\ T_{\mathrm{a,el,out}} &= \frac{2\varepsilon_{\mathrm{el}} T_{\mathrm{w,el,in}} + \left[\varepsilon_{\mathrm{el}} (C_{\mathrm{el}}^{*} - 2) + 2 \right] T_{\mathrm{a,el,in}}}{2+\varepsilon_{\mathrm{el}} C_{\mathrm{el}}^{*}} \end{aligned} \quad . \tag{15}$$

The TEM method can calculate the heat exchanger effectiveness by taking into account the effects of nonuniform airflow. Furthermore, it can take into account the effects of complex tube-side flow circuitry, beyond the reach of available analytical eqns (5)–(8). The number of tube elements used in the TEM method is selected depending on the desired accuracy and the available processor resources. A numerical algorithm for the TEM method was developed. The necessary input parameters are the geometry of the tube-side circuitry, the tube connecting sequence and the number of tubes in each circuit as well as the airflow profile at the inlet. Each tube element in the heat exchanger is assigned three indexes: the first one for the tube element sequence number in the observed tube, the second for the tube sequence number in the observed flow circuit and the third for the flow circuit sequence number in the heat exchanger. The TEM algorithm follows the direction of the tube-side fluid flow, with the outlet temperature of the current tube element being the inlet temperature for the following tube element. Overall, the heat exchanger can be discretized into thousands of tube elements onto which mass and energy conservation equations are applied and solved until reaching the desired level of solution accuracy.

3 RESULTS AND DISCUSSION

3.1 Validation of the analytical method

The results of the TEM method are validated against measurement data collected on the HEX:3R-7C heat exchanger under nonuniform airflow (Fig. 5). The heat exchanger operating conditions are defined by air and water mass flow rates of $\dot{m}_a = 1650$ kg/h and $\dot{m}_w = 800 – 3200$ kg/h, with air and water inlet temperatures of $t_{a,in} = 15°C$ and $t_{w,in} = 60°C$, respectively. Overall, the TEM method achieves very good agreement with experiments. The TEM underestimates the heat exchanger effectiveness in the region of $C^* > 0.4$. Tube-side flow nonuniformity and fin longitudinal heat conduction, both neglected by the TEM method, could be among the possible causes of this discrepancy.

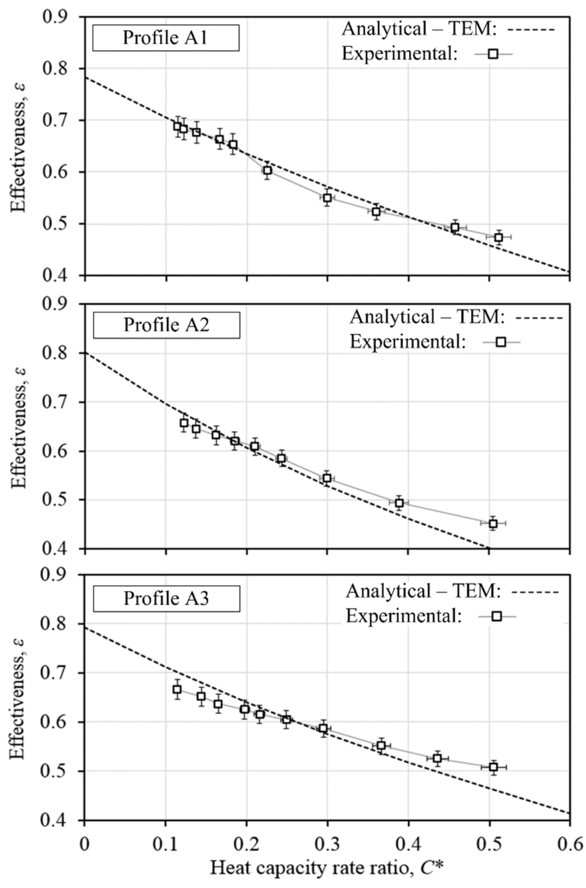

Figure 5: TEM validation: HEX:3R-7C fin-and-tube heat exchanger in nonuniform airflow profiles A1, A2 and A3.

The TEM method is first used to calculate the effectiveness of the HEX:3R-7C heat exchanger with uniform airflow conditions. This is done in order to understand the effect of the flow arrangement on the heat exchanger effectiveness. Fig. 6 shows the heat exchanger effectiveness calculated with the TEM method and compared against the thermal effectiveness of the pure parallelflow heat exchanger (eqn (6)). Fig. 7 shows the comparison between the effectiveness of the HEX:3R-7C heat exchanger and the effectiveness of the single-pass three-tube-row crossflow heat exchanger (eqn (8)). It can be seen that the effectiveness of the HEX:3R-7C heat exchanger is much closer to the effectiveness of the pure parallelflow (Fig. 6) heat exchanger than to the effectiveness of the single-pass three-tube-row crossflow heat exchanger (Fig. 7). This suggests that the Z-shaped tube circuitry of the HEX:3R-7C heat exchanger induces a parallel-crossflow arrangement between the fluid and a consequent loss of thermal performance.

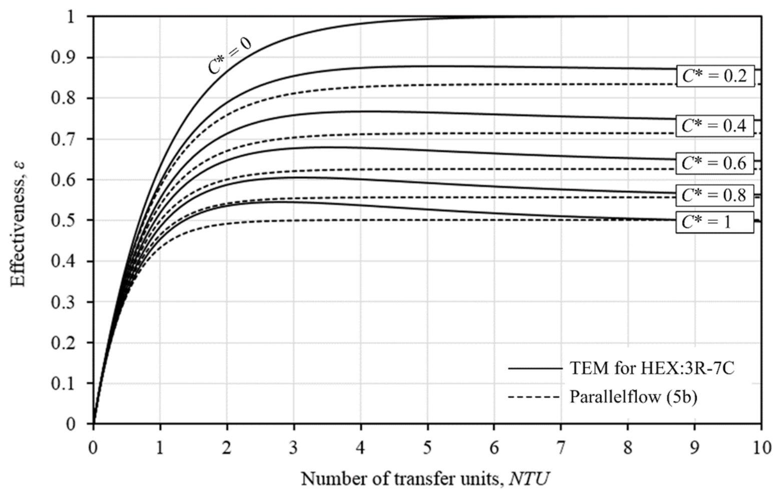

Figure 6: TEM results for the HEX:3R-7C heat exchanger under uniform airflow – comparison against the parallelflow.

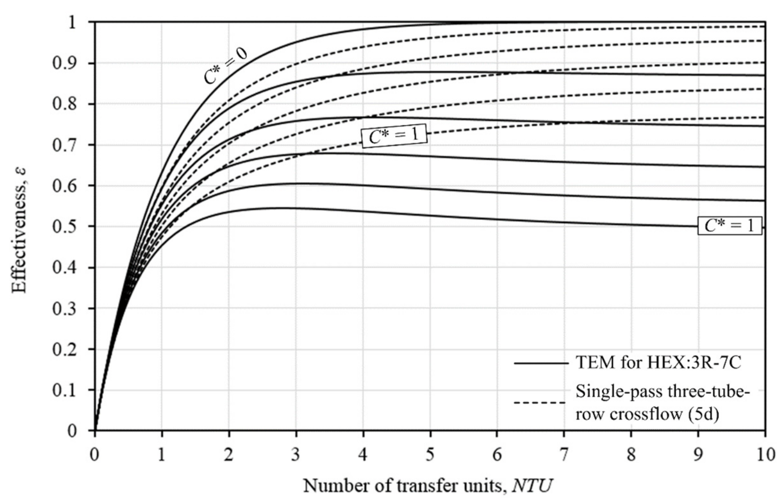

Figure 7: TEM results for the HEX:3R-7C heat exchanger under uniform airflow – comparison against the single-pass three-row crossflow (eqn (8)).

3.2 Heat exchanger effectiveness for nonuniform airflow

The effectiveness of the HEX:3R-7C heat exchanger under nonuniform airflow conditions is calculated using the TEM method. Fig. 8 shows the effectiveness of the HEX:3R-7C heat exchanger operating under nonuniform airflow profile A1 and the comparison against the effectiveness obtained for uniform airflow. Nonuniform airflow profile A1 was generated by blocking access to airflow to the two lowermost flow circuits. Fig. 9 plots the effectiveness deterioration caused by nonuniform airflow A1. The effectiveness deterioration is calculated as the relative difference between the heat exchanger effectiveness for uniform and nonuniform airflow profile, as stated by eqn (3).

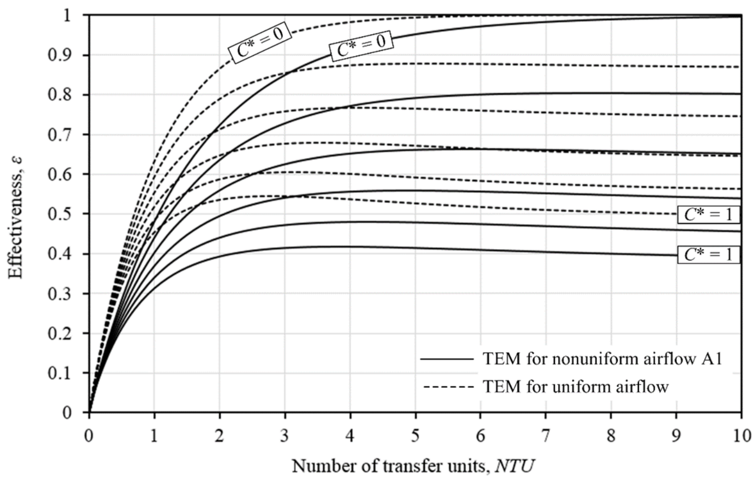

Figure 8: TEM results for the HEX:3R-7C heat exchanger under nonuniform airflow profile A1 – comparison against TEM results for uniform airflow.

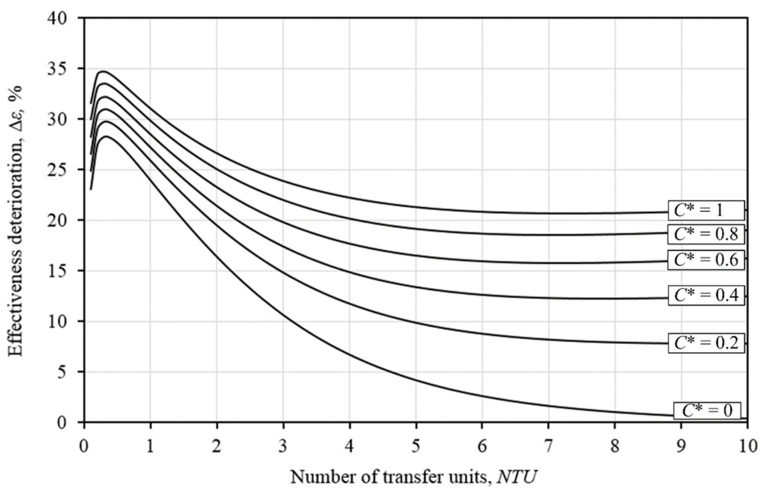

Figure 9: TEM results: effectiveness deterioration caused by nonuniform airflow profile A1.

4 CONCLUSION

A new calculation method for fin-and-tube heat exchangers was presented in this paper – the TEM method. The TEM method was validated against experiments carried out on a heat exchanger operating under nonuniform airflow and very good agreement between predicted and measured values of heat exchanger effectiveness was achieved. The TEM method can be seen as an extension of the standard ε-NTU thermal design method but with the addition of being able to determine the effectiveness of heat exchangers in nonuniform airflow and with complex tube-side flow circuitry. The test subject was a three-row, seven flow circuits fin-and-tube heat exchanger with a total of 38 tubes. The tube-side flow circuitry exhibits a Z-shaped pattern, with water flowing back-and-forth with respect to the incoming airflow. The TEM method revealed that the Z-shaped flow circuitry generates a loss of thermal performance and the resulting effectiveness curves resemble closely the curves of the pure parallelflow rather than those of the single-pass three-row crossflow. Further, the TEM method revealed that nonuniform airflow causes effectiveness deterioration. For the observed nonuniform airflow profiles, the size of the effectiveness deterioration depended on the heat exchanger dimensionless groups, the heat capacity rate ratio C^* and the number of transfer units *NTU*. The method showed that the effectiveness deterioration is the biggest for balanced heat capacity rate ratios ($C^* = 1$), decreases with the decrease of C^* and is the smallest in evaporators and condensers ($C^* = 0$).

The TEM method proved as a valuable tool for the thermal design of fin-and-tube heat exchangers capable of improving the circuitry of the tube-side fluid flow and assessing the effects of airflow nonuniformity on the thermal performance of the heat exchanger.

ACKNOWLEDGEMENT

This work has been fully supported by the Croatian Science Foundation under the project IP-2016-06-4095.

REFERENCES

[1] Kitto, J.B. & Robertson, J.M., Effects of maldistribution of flow on heat transfer equipment performance. *Heat Transfer Engineering,* **10**(1), pp. 18–25, 1989.

[2] Mueller, A.C. & Chiou, J.P., Review of various types of flow maldistribution in heat exchangers. *Heat Transfer Engineering,* **9**(2), pp. 36–50, 1988.

[3] Shah, R.K. & Sekulić, D.P., *Fundamentals of Heat Exchanger Design*, John Wiley & Sons, Inc.: Hoboken, 2003.

[4] Singh, S.K., Mishra, M. & Jha, P.K., Nonuniformities in compact heat exchangers – scope for better energy utilization: A review. *Renewable and Sustainable Energy Reviews*, **40**, pp. 583–596, 2014.

[5] Ranganayakulu, C. & Seetharamu, K.N., The combined effects of wall longitudinal heat conduction, inlet fluid flow nonuniformity and temperature nonuniformity in compact tube-fin heat exchangers: a finite element method. *International Journal of Heat and Mass Transfer*, **42**(2), pp. 263–273, 1999.

[6] Domanski, P.A. & Yashar, D.A., Optimization of finned-tube condensers using an intelligent system. *International Journal of Refrigeration*, **30**(3), pp. 482–488, 2007.

[7] Mao, J.N., Chen, H.X., Jia, H., Wang, Y.Z. & Hu, H.M., Effect of air-side flow maldistribution on thermal-hydraulic performance of the multi-louvered fin and tube heat exchanger. *International Journal of Thermal Sciences*, **73**, pp. 46–57, 2013.

[8] Ranganayakulu, C. & Seetharamu, K.N., *Compact Heat Exchangers: Analysis, Design and Optimization using FEM and CFD Approach*, John Wiley & Sons: USA, 2018.

www.witpress.com, ISSN 1743-3541 (on-line)

[9] Bahman, A.M. & Groll, E.A., Application of interleaved circuitry to improve evaporator effectiveness and COP of a packaged AC system. *International Journal of Refrigeration*, **79**, pp. 114–129, 2017.

[10] Hajabdollahi, H. & Seifoori, S., Effect of flow maldistribution on the optimal design of a cross flow heat exchanger. *International Journal of Thermal Sciences*, **109**, pp. 242–252, 2016.

[11] Yashar, D.A., Domanski, P.A. & Cho, H.H., An experimental and computational study of approach air distribution for a finned-tube heat exchanger. *HVAC&R Research*, **17**(1), pp. 76–85, 2011.

[12] ESDU, Effectiveness-NTU Relationships for the Design and Performance Evaluation of Two-Stream Heat Exchangers, 167 86018, Amendment A, Engineering Science Data Unit Int.: London, pp. 92–107, 1991.

[13] Bačlić, B.S. & Gvozdenac, D.D., Exact explicit equations for some two- and three-pass cross-flow heat exchangers effectiveness. *Heat Exchangers – Thermal Hydraulic Fundamentals and Design*, eds S. Kakac, A.E. Bergles & F. Mayinger, Hemisphere Publishing Corporation: New York, pp. 481–494, 1981.

[14] Gnielinski, G., New equation for heat and mass transfer in turbulent pipe and channel flow. *International Journal of Chemical Engineering*, **16**, pp. 359–368, 1976.

[15] Wang, C.-C., Chi, K.-Y. & Chang, C.-J., Heat transfer and friction characteristics of plain fin-and-tube heat exchangers, part II: Correlation. *International Journal of Heat and Mass Transfer*, **43**(15), pp. 2693–2700, 2000.

[16] Schmidt, T.E., Heat transfer calculations for extended surfaces. *Refrigerating Engineering*, **57**, pp. 351–357, 1949.